

- for ischemic stroke. *Stroke*. 1997; 28: 2109-2118
83. Kwiatkowski TG, Libman RB, Frankel M, et al. Effects of tissue plasminogen activator for acute ischemic stroke at one year. National Institute of Neurological Disorders and Stroke Recombinant Tissue Plasminogen Activator Stroke Study Group. *N Engl J Med*. 1999; 340: 1781-1787
  84. Flemming KD, Brown RD Jr. Acute cerebral infarction caused by aortic dissection: caution in the thrombolytic era. *Stroke*. 1999; 30: 477-478
  85. Iguchi Y, Kimura K, Sakai K, et al. Hyper-acute stroke patients associated with aortic dissection. *Intern Med*. 2010; 49: 543-547
  86. Tomura N, Uemura K, Inugami A, et al. Early CT finding in cerebral infarction: obscuration of the lentiform nucleus. *Radiology*. 1988; 168: 463-467
  87. Truwit CL, Barkovich AJ, Gean-Marton A, et al. Loss of the insular ribbon: another early CT sign of acute middle cerebral artery infarction. *Radiology*. 1990; 176: 801-806
  88. Moulin T, Cattin F, Crepin-Leblond T, et al. Early CT signs in acute middle cerebral artery infarction: predictive value for subsequent infarct locations and outcome. *Neurology*. 1996; 47: 366-375
  89. Gacs G, Fox AJ, Barnett HJ, et al. CT visualization of intracranial arterial thromboembolism. *Stroke*. 1983; 14: 756-762
  90. Pressman BD, Tourje EJ, Thompson JR. An early CT sign of ischemic infarction: increased density in a cerebral artery. *AJR Am J Roentgenol*. 1987; 149: 583-586
  91. Schuierer G, Huk W. The unilateral hyperdense middle cerebral artery: an early CT-sign of embolism or thrombosis. *Neuroradiology*. 1988; 30: 120-122
  92. Leys D, Pruvo JP, Godefroy O, et al. Prevalence and significance of hyperdense middle cerebral artery in acute stroke. *Stroke*. 1992; 23: 317-324
  93. Barber PA, Demchuk AM, Hudon ME, et al. Hyperdense sylvian fissure MCA "dot" sign: A CT marker of acute ischemia. *Stroke*. 2001; 32: 84-88
  94. Leary MC, Kidwell CS, Villablanca JP, et al. Validation of computed tomographic middle cerebral artery "dot" sign: an angiographic correlation study. *Stroke*. 2003; 34: 2636-2640
  95. Koga M, Saku Y, Toyoda K, et al. Reappraisal of early CT signs to predict the arterial occlusion site in acute embolic stroke. *J Neurol Neurosurg Psychiatry*. 2003; 74: 649-653
  96. Wardlaw JM, Mielke O. Early signs of brain infarction at CT: observer reliability and outcome after thrombolytic treatment: systematic review. *Radiology*. 2005; 235: 444-453
  97. Ogawa A, Mori E, Minematsu K, et al. Randomized trial of intraarterial infusion of urokinase within 6 hours of middle cerebral artery stroke: the middle cerebral artery embolism local fibrinolytic intervention trial (MELT) Japan. *Stroke*. 2007; 38: 2633-2639
  98. 小川彰. 画像標準化及び判定法標準化. 主任研究者小川彰. 超急性期脳塞栓症に対する局所線溶療法の効果に関する臨床研究「超急性期脳梗塞に対する局所線溶療法の効果に関する臨床研究 —超急性期局所線溶療法多施設共同ランダム化比較試験—」. 平成 14 年度厚生労働科学研究費補助金による効果的医療技術の確立推進臨床研究事業報告書. 岩手医科大学医学部, 岩手, 2002, pp.41-44
  99. von Kummer R. Effect of training in reading CT scans on patient selection for ECASS II. *Neurology*. 1998; 51: S50-S52
  100. ASIST-Japan 実践ガイドライン策定委員会. 急性期脳梗塞画像診断実践ガイドライン. 南江堂, 東京, 2007
  101. Barber PA, Demchuk AM, Zhang J, et al. Validity and reliability of a quantitative computed tomography score in predicting outcome of hyperacute stroke before thrombolytic therapy. ASPECTS Study Group. Alberta Stroke Programme Early CT Score. *Lancet*. 2000; 355: 1670-1674
  102. Pexman JH, Barber PA, Hill MD, et al. Use of the Alberta Stroke Program Early CT Score (ASPECTS) for assessing CT scans in patients with acute stroke. *AJNR Am J Neuroradiol*. 2001; 22: 1534-1542.
  103. Hill MD, Barber PA, Demchuk AM, et al. Acute intravenous-intra-arterial revascularization therapy for severe ischemic stroke. *Stroke*. 2002; 33: 279-282
  104. Hirano T, Yonehara T, Inatomi Y, et al. Presence of early ischemic changes on computed tomography depends on severity and the duration of hypoperfusion: a single photon emission-computed tomographic study. *Stroke*. 2005; 36: 2601-2608
  105. Ezzeddine MA, Lev MH, McDonald CT, et al. Extent of early ischemic changes on computed tomography (CT) before thrombolysis: prognostic value of the Alberta Stroke Program Early CT Score in ECASS II. *Stroke*. 2002; 33: 959-966
  106. Schramm P, Schellinger PD, Klotz E, et al. Comparison of perfusion computed tomography and

- computed tomography angiography source images with perfusion-weighted imaging and diffusion-weighted imaging in patients with acute stroke of less than 6 hours' duration. *Stroke*. 2004; 35: 1652-1658
107. Larrue V, von Kummer R, Del Zoppo G, et al. Hemorrhagic transformation in acute ischemic stroke. Potential contributing factors in the European Cooperative Acute Stroke Study. *Stroke*. 1997; 28: 957-960
  108. Patel SC, Levine SR, Tilley BC, et al. Lack of clinical significance of early ischemic changes on computed tomography in acute stroke. *JAMA*. 2001; 286: 2830-2838
  109. Demchuk AM, Hill MD, Barber PA, et al. Importance of early ischemic computed tomography changes using ASPECTS in NINDS rtPA Stroke Study. *Stroke*. 2005; 36: 2110-2115
  110. Dzialowski I, Hill MD, Coutts SB, et al. Extent of early ischemic changes on computed tomography (CT) before thrombolysis: prognostic value of the Alberta Stroke Program Early CT Score in ECASS II. *Stroke*. 2006; 37: 973-978
  111. Hirano T, Sasaki M, Tomura N, et al. Low Alberta Stroke Program Early Computed Tomography Score within 3 hours of onset predicts subsequent symptomatic intracranial hemorrhage in patients treated with 0.6 mg/kg alteplase. *J Stroke Cerebrovasc Dis*. 2011 Jul 5. [Epub ahead of print]
  112. Warach S, Chien D, Li W, et al. Fast magnetic resonance diffusion-weighted imaging of acute human stroke. *Neurology*. 1992; 42: 1717-1723
  113. Warach S, Gaa J, Siewert B, et al. Acute human stroke studied by whole brain echo planar diffusion-weighted magnetic resonance imaging. *Ann Neurol*. 1995; 37: 231-241
  114. Lutsep HL, Albers GW, DeCrespigny A, et al. Clinical utility of diffusion-weighted magnetic resonance imaging in the assessment of ischemic stroke. *Ann Neurol*. 1997; 41: 574-580
  115. Barber PA, Darby DG, Desmond PM, et al. Prediction of stroke outcome with echoplanar perfusion- and diffusion-weighted MRI. *Neurology*. 1998; 51: 418-426
  116. Thomalla G, Rossbach P, Rosenkranz M, et al. Negative fluid-attenuated inversion recovery imaging identifies acute ischemic stroke at 3 hours or less. *Ann Neurol*. 2009; 65: 724-732
  117. Aoki J, Kimura K, Iguchi Y, et al. Intravenous thrombolysis based on diffusion-weighted imaging and fluid-attenuated inversion recovery mismatch in acute stroke patients with unknown onset time. *Cerebrovasc Dis*. 2011; 31: 435-441
  118. Kidwell CS, Chalela JA, Saver JL, et al. Comparison of MRI and CT for detection of acute intracerebral hemorrhage. *JAMA*. 2004; 292: 1823-1830
  119. Arnould MC, Grandin CB, Peeters A, et al. Comparison of CT and three MR sequences for detecting and categorizing early (48 hours) hemorrhagic transformation in hyperacute ischemic stroke. *AJNR Am J Neuroradiol*. 2004; 25: 939-944
  120. Fiebach JB, Schellinger PD, Gass A, et al. Stroke magnetic resonance imaging is accurate in hyperacute intracerebral hemorrhage: a multicenter study on the validity of stroke imaging. *Stroke*. 2004; 35: 502-506
  121. Cho KH, Kim JS, Kwon SU, et al. Significance of susceptibility vessel sign on T2\*-weighted gradient echo imaging for identification of stroke subtypes. *Stroke*. 2005; 36: 2379-2383
  122. Sasaki M, Ida M, Yamada K, et al. Standardizing display conditions of diffusion-weighted images using concurrent b0 images: a multi-vendor multi-institutional study. *Magn Reson Med Sci*. 2007; 6: 133-137
  123. Barber PA, Hill MD, Eliasziw M, et al. Imaging of the brain in acute ischaemic stroke: comparison of computed tomography and magnetic resonance diffusion-weighted imaging. *J Neurol Neurosurg Psychiatry*. 2005; 76: 1528-1533
  124. Nezu T, Koga M, Nakagawara J, et al. Early ischemic change on CT versus diffusion-weighted imaging for patients with stroke receiving intravenous recombinant tissue-type plasminogen activator therapy: stroke acute management with urgent risk-factor assessment and improvement (SAMURAI) rt-PA registry. *Stroke*. 2011; 42: 2196-2200
  125. Marks MP, Tong DC, Beaulieu C, et al. Evaluation of early reperfusion and i.v. tPA therapy using diffusion- and perfusion-weighted MRI. *Neurology*. 1999; 52: 1792-1798
  126. Kidwell CS, Saver JL, Mattiello J, et al. Thrombolytic reversal of acute human cerebral ischemic injury shown by diffusion/perfusion magnetic resonance imaging. *Ann Neurol*. 2000; 47: 462-469
  127. Ma H, Parsons MW, Christensen S, et al: EXTEND investigators. A multicentre, randomized, double-blinded, placebo-controlled Phase III study to investigate EXtending the time for Thrombolysis in Emergency Neurological Deficits (EXTEND). *Int J Stroke*. 2012; 7: 74-80
  128. Latchaw RE, Alberts MJ, Lev MH, et al. Recommendations for imaging of acute ischemic stroke: a

- scientific statement from the American Heart Association. *Stroke*. 2009; 40: 3646-3678
129. Schellinger PD, Thomalla G, Fiehler J, et al. MRI-based and CT-based thrombolytic therapy in acute stroke within and beyond established time windows: an analysis of 1210 patients. *Stroke*. 2007; 38: 2640-1645
  130. Nezu T, Koga M, Kimura K, et al. Pretreatment ASPECTS on DWI predicts 3-month outcome following rt-PA: SAMURAI rt-PA Registry. *Neurology*. 2010; 75: 555-561
  131. Kimura K, Iguchi Y, Shibazaki K, et al. Large ischemic lesions on diffusion-weighted imaging done before intravenous tissue plasminogen activator thrombolysis predicts a poor outcome in patients with acute stroke. *Stroke*. 2008; 39: 2388-2391
  132. Fiehler J, Albers GW, Boulanger JM, et al; MR STROKE Group. Bleeding risk analysis in stroke imaging before thrombolysis (BRASIL): pooled analysis of T2\*-weighted magnetic resonance imaging data from 570 patients. *Stroke*. 2007; 38: 2738-2744
  133. Kimura K, Iguchi Y, Shibazaki K, et al. M1 susceptibility vessel sign on T2\* as a strong predictor for no early recanalization after IV-t-PA in acute ischemic stroke. *Stroke*. 2009; 40: 3130-3132
  134. Kimura K, Sakamoto Y, Aoki J, et al. Clinical and MRI predictors of no early recanalization within 1 hour after tissue-type plasminogen activator administration. *Stroke*. 2011; 42: 3150-3155
  135. Ueda T, Hatakeyama T, Kumon Y, et al. Evaluation of risk of hemorrhagic transformation in local intra-arterial thrombolysis in acute ischemic stroke by initial SPECT. *Stroke*. 1994; 25: 298-303
  136. Alexandrov AV, Molina CA, Grotta JC, et al. Ultrasound-enhanced systemic thrombolysis for acute ischemic stroke. *New Engl J Med*. 2004; 351: 2170-2178
  137. Eggers J, Konig IR, Koch B, et al. Sonothrombolysis with transcranial color-coded sonography and recombinant tissue-type plasminogen activator in acute middle cerebral artery main stem occlusion: results from a randomized study. *Stroke*. 2008; 39: 1470-1475
  138. del Zoppo GJ, Poeck K, Pessin MS, et al. Recombinant tissue plasminogen activator in acute thrombotic and embolic stroke. *Ann Neurol*. 1992; 32: 78-86
  139. Linfante I, Llinas RH, Selim M, et al. Clinical and vascular outcome in internal carotid artery versus middle cerebral artery occlusions after intravenous tissue plasminogen activator. *Stroke*. 2002; 33: 2066-2071
  140. Saqqur M, Uchino K, Demchuk AM, et al. Site of arterial occlusion identified by transcranial Doppler predicts the response to intravenous thrombolysis for stroke. *Stroke*. 2007; 38: 948-954
  141. Rubiera M, Ribo M, Delgado-Mederos R, et al. Tandem internal carotid artery/middle cerebral artery occlusion: an independent predictor of poor outcome after systemic thrombolysis. *Stroke*. 2006; 37: 2301-2305
  142. Nakashima T, Toyoda K, Koga M, et al. Arterial occlusion sites on magnetic resonance angiography influence the efficacy of intravenous low-dose (0.6 mg/kg) alteplase therapy for ischaemic stroke. *Int J Stroke*. 2009; 4: 425-431
  143. Kimura K, Iguchi Y, Shibazaki K, et al. Early recanalization rate of major occluded brain arteries after intravenous tissue plasminogen activator therapy using serial magnetic resonance angiography studies. *Eur Neurol*. 2009; 62: 287-292
  144. Koga M, Toyoda K, Nakashima T, et al. Carotid duplex ultrasonography can predict outcome of intravenous alteplase therapy for hyperacute stroke. *J Stroke Cerebrovasc Dis*. 2011; 20: 24-29
  145. Hirano T, Sasaki M, Mori E, et al. Residual vessel length on magnetic resonance angiography identifies poor responders to alteplase in acute middle cerebral artery occlusion patients: exploratory analysis of the Japan Alteplase Clinical Trial II. *Stroke*. 2010; 41: 2828-2833.
  146. 宮本享ら. 循環器病研究委託費 20 指 2・循環器病研究開発費 22-4-1 分担研究「重症脳卒中における生命倫理に関する研究」からの答申書, 2012
  147. Yong M, Kaste M. Association of characteristics of blood pressure profiles and stroke outcomes in the ECASS-II trial. *Stroke*. 2008; 39: 366-372
  148. Ahmed N, Wahlgren N, Brainin M, et al. Relationship of blood pressure, antihypertensive therapy, and outcome in ischemic stroke treated with intravenous thrombolysis: retrospective analysis from Safe Implementation of Thrombolysis in Stroke-International Stroke Thrombolysis Register (SITS-ISTR). *Stroke*. 2009; 40: 2442-2449
  149. Tomii Y, Toyoda K, Nakashima T, et al. Effects of hyperacute blood pressure and heart rate on stroke outcomes after intravenous tissue plasminogen activator. *J Hypertens*. 2011; 29: 1980-1987
  150. 日本高血圧学会高血圧治療ガイドライン作成委員会. 高血圧治療ガイドライン 2009. 日本高血圧学会, 東京, 2009, pp90-94
  151. Zinkstok SM, Roos YB, on behalf of the ARTIS investigators. Early administration of aspirin in

- patients treated with alteplase for acute ischaemic stroke: a randomized controlled trial. *Lancet*. 2012; 380: 731-737
152. Barreto AD, Alexandrov AV, Lyden P, et al. The argatroban and tissue-type plasminogen activator stroke study: final results of a pilot safety study. *Stroke*. 2012; 43: 770-775
  153. Lopez-Yunez AM, Bruno A, Williams LS, et al. Protocol violations in community-based rTPA stroke treatment are associated with symptomatic intracerebral hemorrhage. *Stroke*. 2001; 32: 12-16
  154. Morgenstern LB, Hemphill JC, 3rd, Anderson C, et al. Guidelines for the management of spontaneous intracerebral hemorrhage: a guideline for healthcare professionals from the American Heart Association/American Stroke Association. *Stroke*. 2010; 41: 2108-2129
  155. Furlan A, Higashida R, Wechsler L, et al : Intra-arterial prourokinase for acute ischemic stroke. The PROACT II study: a randomized controlled trial. *Prolyse in Acute Cerebral Thromboembolism*. *JAMA*. 1999; 282 : 2003-2011
  156. Lisboa RC, Jovanovic BD, Alberts MJ. Analysis of the safety and efficacy of intra-arterial thrombolytic therapy in ischemic stroke. *Stroke*. 2002; 33: 2866-2871
  157. Lansberg MG, O'Donnell MJ, Khatri P, et al. Antithrombotic and Thrombolytic Therapy for Ischemic Stroke : Antithrombotic Therapy and Prevention of Thrombosis, 9th ed: American College of Chest Physicians Evidence-Based Clinical Practice Guideline. *Chest*. 2012; 141; e601S-e636S
  158. Lewandowski CA, Frankel M, Tomsick TA, et al. Combined intravenous and intra-arterial r-TPA versus intra-arterial therapy of acute ischemic stroke: Emergency Management of Stroke (EMS) Bridging Trial. *Stroke*. 1999; 30: 2598-2605
  159. Combined intravenous and intra-arterial recanalization for acute ischemic stroke: the Interventional Management of Stroke Study. *Stroke*. 2004; 35: 904-911
  160. The IMS II Trial Investigators. The Interventional Management of Stroke (IMS) II Study. *Stroke*. 2007; 38: 2127-2135
  161. Higashida RT, Furlan AJ, Roberts H, et al. Trial design and reporting standards for intra-arterial cerebral thrombolysis for acute ischemic stroke. *Stroke*. 2003; 34: e109-e137
  162. 一般社団法人日本脳卒中学会. Merci リトリーバー適正治療指針について. Available from: <http://www.jsts.gr.jp/img/merc.pdf>
  163. 一般社団法人日本脳卒中学会. Penumbra システム適正治療指針について. Available from: <http://www.jsts.gr.jp/img/penumbra.pdf>
  164. Smith WS, Sung G, Starkman S, et al. Safety and Efficacy of Mechanical Embolectomy in Acute Ischemic Stroke Result of the MERCI Trial. *Stroke*. 2005; 36: 1432-1440
  165. Smith WS, Sung G, Saver J, et al. Mechanical Thrombectomy for Acute Ischemic Stroke: Final Results of the Multi MERCI Trial. *Stroke*. 2008; 39: 1205-1212
  166. Shi ZS, Loh Y, Walker G, et al. Endovascular thrombectomy for acute ischemic stroke in failed intravenous tissue plasminogen activator versus non-intravenous tissue plasminogen activator patients: revascularization and outcomes stratified by the site of arterial occlusions. *Stroke*. 2010; 41: 1185-1192
  167. The penumbra pivotal stroke trial. Safety and effectiveness of a new generation of mechanical devices for clot removal in intracranial large vessel occlusive disease. *Stroke*. 2009; 40: 2761-2768.
  168. Goyal M, Menon BK, Coultis SB, et al. Effect of baseline CT scan appearance and time to recanalization on clinical outcomes in endovascular thrombectomy of acute ischemic strokes. *Stroke*. 2011; 42: 93-97
  169. Tarr R, Hsu D, Kulcsar Z, et al. The POST trial: initial post-market experience of the Penumbra system: revascularization of large vessel occlusion in acute ischemic stroke in the United States and Europe. *J NeuroIntervent Surg*. 2010; 2: 341-344
  170. Saver JL, Jahan R, Levy EI, et al. Solitaire flow restoration device versus the Merci Retriever in patients with acute ischaemic stroke (SWIFT): a randomised, parallel-group, non-inferiority trial. *Lancet*. 2012; 380: 1241-1249
  171. Nogueira RG, Lutsep HL, Gupta R, et al. Trevo versus Merci retrievers for thrombectomy revascularisation of large vessel occlusions in acute ischaemic stroke (TREVO 2): a randomised trial. *Lancet*. 2012; 380: 1231-1240
  172. Nahab F, Walker GA, Dion JE, et al. Safety of Periprocedural Heparin in Acute Ischemic Stroke Endovascular Therapy: The Multi MERCI Trial. *J Stroke Cerebrovasc Dis*. 2011 Jun 1. [Epub ahead of print]

## 第二版における推奨項目のおもな変更点

推奨項目	初回版	第二版	
● 治療開始可能時間	発症から3時間以内に	発症から4.5時間以内に	
● 治療の適応, 表3			
脳梗塞の既往	3ヵ月以内の脳梗塞は禁忌	最終発症から1ヵ月以内の脳梗塞は、適応外 ※直近の脳梗塞の出血性変化がCT上で高吸収域所見として残っている場合は、1ヵ月を過ぎていても適応外	○
胸部大動脈解離, 胸部大動脈瘤	記載なし	胸部大動脈解離が強く疑われる場合は適応外, 胸部大動脈瘤の存在が判明している場合は慎重投与	○
凝固マーカーの異常値	ワーファリン内服中 PT-INR >1.7, ヘパリン投与中APTTの延長は、禁忌	抗凝固療法中ないし凝固異常症において、PT-INRが1.7を超える場合やaPTTが前値の1.5倍を超える場合は、適応外	○
画像所見	頭部CTで広汎な早期虚血性変化は禁忌	頭部CTやMRIでの広汎な早期虚血性変化の存在は、適応外	○
年齢	75歳以上は慎重投与	81歳以上は慎重投与	○
3ヵ月以内の心筋梗塞	記載なし	慎重投与	○
NIHSS値	23以上は慎重投与	26以上は慎重投与	○
JCS	100以上は慎重投与	記載なし	○
軽症例や症状が急速に改善して軽症化する症例	確認事項として記載	慎重投与	○
痙攣	禁忌	慎重投与 ※既往歴などからてんかんの可能性が高ければ適応外。	○
脳動脈瘤・頭蓋内腫瘍・脳動脈静脈奇形・もやもや病	禁忌	慎重投与	○
● 発症より来院までの対応 (市民啓発, 救急隊員の病院前救護)	記載なし	アルテプラゼ静注療法を適切に行うために、市民啓発や救急隊員の病院前救護の改善に努め、患者の迅速な受診を促す	
● 適応の判定と説明・同意 (説明・同意)	治療による利益・不利益を本人, 家族に十分説明し, 理解を得た上での同意が必要である。	適応例に対しては, 利益・不利益について可能な限り患者ないし代諾者に説明し, 同意を得ることが望ましいが, それは必須条項ではなく, 代諾者不在であるがゆえに患者が本治療を受けられないような事態は避けるべきである。 慎重投与例に対しては, 患者ないし代諾者への十分な説明に基づく同意取得が必要である。代諾者が不在の場合に備えて, 各施設における最近の治療成績に基づいた本治療法の可否に関する方針を, 予め確定しておく。その上で代諾者不在時には, 診療チームによる合議によって適切と判断された場合に限り, 治療し得る。	
● 投与開始後の管理, 表12			
SCUないしそれに準じた病棟での管理	最短でも治療開始後36時間まで	治療開始後24時間以上	
治療開始後の24時間の抗血栓療法	禁止 (表13に記載)	治療開始後の24時間は, 抗血栓療法の制限が重要である。基本的には, 24時間以内は抗凝固薬, 抗血小板薬, 血栓溶解薬を投与しない。ただし血管造影時や深部静脈血栓症予防目的のヘパリン(1万単位以下)は使用可能であるが, 頭蓋内出血の危険性を考慮する必要がある。	※
● 血管内治療 (機械的再開通療法)	機械的再開通療法の記載なし	発症後8時間以内の機械的再開通療法は, アルテプラゼ静注療法の非適応および無効例に限って承認されたが, その有効性・安全性は未だに検証中であることに留意する。	

○ : 初回版がアルテプラゼの添付文書に沿って記載されており, 第二版の記載は添付文書と異なる。

※ : 添付文書にはヘパリン量を「5000単位を超えない」と記載されている。

## 本治療指針で用いられた英略語

## 1. 一般名詞

略語	正式名称
ADC	apparent diffusion coefficient
aPTT	activated partial thromboplastin time
CT	computed tomography
CTA	computed tomographic angiography
DWI	diffusion-weighted image
EIC	early ischemic change
FLAIR	fluid-attenuated inversion recovery
LIF	local fibrinolytic therapy
MRA	magnetic resonance angiography
MRI	magnetic resonance imaging
PH	parenchymal hematoma
PSLS	prehospital stroke life support
PSS	prehospital stroke scale
PT-INR	prothrombin time, international normalized ratio
PWI	perfusion-weighted imaging
rt-PA	recombinant tissue-type plasminogen activator
SCU	stroke care unit
SPECT	single photon emission computed tomography
TC-CFI	transcranial color-flow imaging
TCD	transcranial Doppler

## 2. 試験名, 団体名など

略語	正式名称
ASIST-Japan	Acute Stroke Imaging Standardization Group-Japan
ASPECTS	Alberta Stroke Program Early CT Score
ATLANTIS	Alteplase Thrombolysis for Acute Noninterventional Therapy in Ischemic Stroke
DEFUSE	Diffusion and Perfusion Imaging Evaluation for Understanding Stroke Evolution
DIAS-II	Desmoteplase in Acute Ischemic Stroke II
EXTEND	EXtending the time for Thrombolysis in Emergency Neurological Deficits
ECASS	European Cooperative Acute Stroke Study
EPITHET	Echoplanar Imaging Thrombolysis Evaluation Trial
IST-3	Third International Stroke Trial
J-ACT (II)	Japan Alteplase Clinical Trial
J-MARS	Japan post-Marketing Alteplase Registration Study
KPSS	Kurashiki Prehospital stroke scale
MELT-Japan	Middle Cerebral Artery Embolism Local Fibrinolytic Intervention Trial-Japan
MERCI	Mechanical Embolus Removal in Cerebral Ischemia
mRS	modified Rankin scale
NIHSS	National Institutes of Health stroke scale
NINDS	National Institute of Neurological Disorders and Stroke
OHS	Oxford Handicap Score
PROACT II	Prolyse in Acute Cerebral Thromboembolism II
SAMURAI	Stroke Acute Management with Urgent Risk-factor Assessment and Improvement
SITS-ISTR	Safe Implementation of Treatments in Stroke-International Stroke Thrombolysis Registry
SWIFT	SOLITAIRE™ FR With the Intention For Thrombectomy
TIMI	Thrombolysis In Myocardial Infarction
TREVO 2	Thrombectomy REvascularization of large Vessel Occlusions in acute ischemic stroke 2
UCAS Japan	Unruptured Cerebral Aneurysm Study of Japan
VISTA	Virtual International Stroke Trials Archive

## Surgical Treatment for Carotid Stenoses with Highly Calcified Plaques

Hiroyuki Katano, MD, PhD,\*† Mitsuhiro Mase, MD, PhD,\* Yusuke Nishikawa, MD, PhD,\*  
and Kazuo Yamada, MD, PhD\*

**Background:** The aim of this study was to clarify both the present status of treatment for carotid stenosis with highly calcified plaques and the appropriate treatment. **Methods:** A total of 140 consecutive treatments for carotid stenoses (carotid endarterectomy [CEA]:carotid artery stenting [CAS] 81:59) were enrolled in the study. We classified the patients into low-calcified plaque (LCP) and high-calcified plaque (HCP) groups by calcium score, determined by a receiver operating characteristic analysis, and we compared the results after both treatments. **Results:** The mean degree of residual stenosis and improvement rates of the stenosis after CAS for the HCP group were  $9.7\% \pm 13.3\%$  and  $87.0\% \pm 16.8\%$ , respectively, whereas those for the LCP group were  $1.7\% \pm 6.1\%$  and  $97.9\% \pm 7.9\%$  (both  $P < .001$ ). A multiple logistic regression analysis revealed that only the calcium score was an independent pre-CAS predictor of residual stenosis. Restenosis at 6 months was observed frequently in the HCP group after both CAS and CEA (18.8% and 20.0%, respectively). Cerebral hyperperfusion syndrome was observed in 2 cases of CAS, 1 for each plaque group. The 30-day and 6-month rates for any stroke or death after CAS were 2.3% and 12.5% for the LCP and HCP groups, respectively, whereas those after CEA were 1.6% and 0%. **Conclusions:** Carotid stenoses with HCP (calcium score  $\geq 420$ ) treated by CAS showed a disadvantage in the degree of stent expansion compared to carotid stenoses with LCP, suggesting that CEA may be recommended as a surgical option. **Key Words:** Calcification—carotid artery stenting—carotid endarterectomy—carotid stenosis.

© 2013 by National Stroke Association

After the approval of self-expanding stents with filter protection devices by the Japanese Ministry of Health Labor and Welfare in 2008,<sup>1,2</sup> the rate of postoperative ischemic complications with so-called “soft” vulnerable lipid-rich plaques temporarily increased in patients with

carotid artery stenting (CAS) treated in Japan. The rate decreased after the application of appropriate embolic protection devices.<sup>3,4</sup> Therefore, one of the remaining problems concerning the treatment of carotid stenosis may concern instead the so-called “hard plaques” with calcification.

In a previous study, our pathologic and radiologic assessments suggested that severely calcified plaque might prevent the expansion of carotid stents and therefore affect the results of CAS,<sup>5,6</sup> and we recommended that physicians conduct a preoperative analysis of carotid plaque using the Agatston calcium score with multidetector computed tomography angiography (MDCTA).<sup>7</sup>

Nonaka et al<sup>8</sup> warned that calcification at carotid bifurcations is an independent risk factor for prolonged hypotension after CAS that might relate to periprocedural ischemic events. They described how plaque calcification

From the \*Departments of Neurosurgery; and †Medical Informatics and Integrative Medicine, Nagoya City University Graduate School of Medical Sciences, Nagoya, Japan.

Received October 23, 2012; revision received November 24, 2012; accepted November 28, 2012.

Address correspondence to Hiroyuki Katano, MD, Department of Neurosurgery, Nagoya City University Graduate School of Medical Sciences, 1 Kawasumi, Mizuho-cho, Mizuho-ku, Nagoya 467-8601, Japan. E-mail: katano@med.nagoya-cu.ac.jp.

1052-3057/\$ - see front matter

© 2013 by National Stroke Association

<http://dx.doi.org/10.1016/j.jstrokecerebrovasdis.2012.11.019>

San Mateo, CA) with preoperative MDCTA data. Calcium scores were calculated as the products of the areas of calcified lesions and the weighted signal intensity scalars, dependent on the maximal Hounsfield unit (HU) value within the lesion (scalar = 1 if 130-199 HU, 2 if 200-299, 3 if 300-399, and 4 if  $\geq 400$ ). The analysis of the degrees of stenoses before and after the operation was also performed with MDCTA using the NASCET method.<sup>12</sup> The ROC analysis revealed that the optimal cutoff value for the calcium score was 420 for postoperative residual stenosis  $>25\%$  after CAS (sensitivity 0.750; specificity 0.764; pseudopositive ratio 0.236; Fig 1). On the basis of this ROC analysis, we divided all cases for further assessment into an HCP group with calcium scores  $\geq 420$  and an LCP group with calcium scores  $< 420$ .

#### *Diffusion-weighted Images of Magnetic Resonance Imaging*

Magnetic resonance imaging including diffusion-weighted (DW) images was performed to detect newly developed ischemia as a high-intensity spot (HIS) with a 1.5-T imaging system (Gyroscan Integra; Philips) using a single-shot diffusion echo planar imaging (EPI) sequence with the following parameters: TR 2917 ms, TE 83 ms, flip angle  $90^\circ$ , 5.0-mm section thickness, field of view 23.0 cm, number of excitations 1, b value = 0, and  $1000 \text{ s/mm}^2$ .

#### *Residual Stenosis, Improvement Rate, and Restenosis/In-stent Restenosis*

Residual stenosis was also measured using the NASCET method<sup>12</sup> and stenosis of  $>25\%$  was counted. The improvement rate was calculated as  $[100 (\text{preoperative}$

degree of stenosis–postoperative degree of stenosis)/preoperative degree of stenosis]. A multiple logistic regression analysis was performed to find independent preoperative predictors of residual stenosis. Six months after the operations, both restenosis after CEA and in-stent restenosis after CAS of  $>25\%$  were counted. The latter was detected as a low-density defect in the lumen inside the stent wall in any sagittal or axial multiplanar reconstruction (MPR) images of MDCTA.

#### *Single-photon Emission Computed Tomography and Hyperperfusion*

Postoperative N-isopropyl-p-[<sup>123</sup>I]-iodoamphetamine (IMP)–single-photon emission computed tomography was performed using the autoradiography (ARG) method and checked for the occurrence of hyperperfusion using a dual-head gamma camera system (E.CAM; Siemens, Erlangen, Germany) equipped with high-resolution fan-beam collimators. For data acquisition, we used a  $128 \times 128$  matrix for 36 steps of  $5^\circ$ , field of view 422 mm, and 5-mm slice thickness. Postoperative hyperperfusion was defined as a regional cerebral blood flow (rCBF) increase of  $>100\%$ <sup>17</sup> compared to the preoperative values in  $>1$  region of interest (ROI) analyzed with a 3-dimensional stereotactic ROI template (3DSRT; Fuji Film RI Pharma Co, Tokyo, Japan).<sup>18,19</sup> Cerebral hyperperfusion syndrome (CHS) was defined as having symptoms such as seizure, deterioration of consciousness level, focal neurologic signs with or without postoperative intracerebral hemorrhage (ICH), and no evidence of new postoperative ischemia.

#### *Statistical Analysis*

All statistical evaluations were performed with Statview (version 5.0; SAS Inc, Cary, NC) and StatMate III software (ATMS; Tokyo), and all results are presented as mean  $\pm$  standard deviation. The ROC analysis was performed to set the cutoff value of the calcium scores in the prediction of residual stenosis after CAS. The Chi-square test with the Yates correction and the Mann-Whitney *U* test were used for comparison. For the multivariate analysis, a logistic regression model was used.  $P < .05$  was considered statistically significant.

## Results

The characteristics for all cases are shown in Table 1. There were no significant differences between the CEA and CAS groups concerning gender, degree of stenosis, and the percentage of symptomatic cases and calcium scores, except for a slight difference in the mean ages of the groups because of the application of the surgical indication of the SAPPHERE study.<sup>14</sup>

The HCP group consisted of 20 (24.7%) CEA cases and 16 (27.1%) CAS cases (Table 2). The mean residual degree

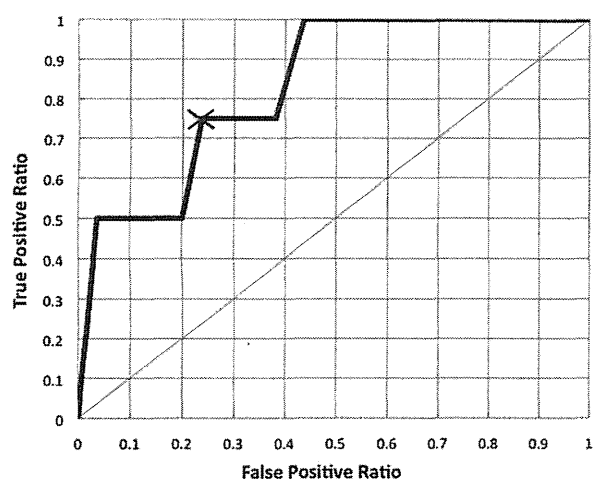


**Figure 1.** Receiver operating characteristic (ROC) analysis for the prediction of postoperative residual stenosis of  $>25\%$  after carotid artery stenting. The optimal cutoff value of the calcium score was revealed to be 420 with a sensitivity of 0.750, specificity of 0.764, pseudopositive ratio of 0.236, and an area under the curve of 0.746.

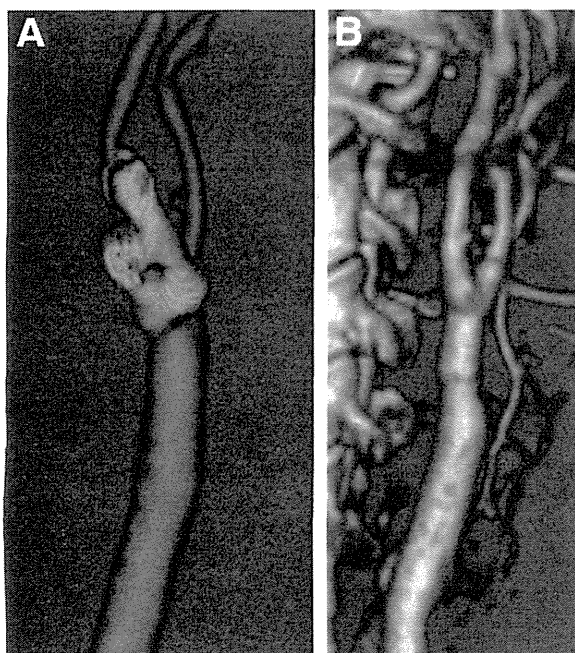


**Figure 2.** A right carotid endarterectomy case of a 76-year-old woman with 75% carotid stenosis. (A) Preoperative computed tomographic angiography revealed a high-calcified plaque at the right carotid bifurcation (calcium score 625.9). (B) Postoperative computed tomographic angiography revealed excellent dilatation with disappearance of calcification.

Transluminal Angioplasty Study (CAVATAS) who were found to have severe stenosis at 1 year. In addition, Aronow et al<sup>21</sup> observed that there was a greater risk of neurologic death or stroke after CAS when the final residual diameter stenosis was >30%, and Randall et al<sup>22</sup> also pointed out the importance of residual stenosis >50% as a possible risk factor for recurrent stroke events.

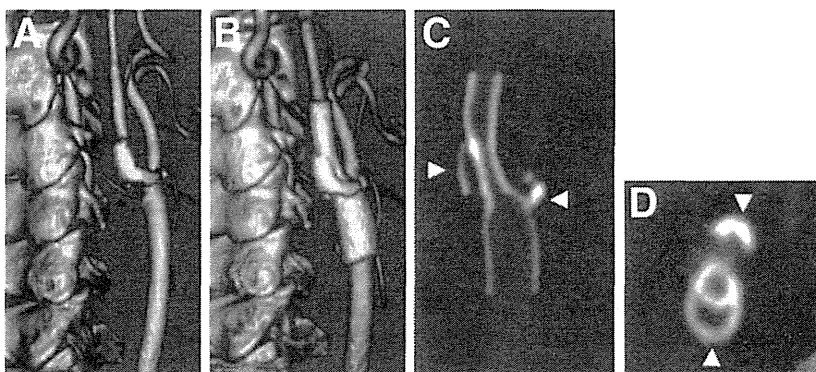
To counterbalance the external pressure created by severe calcification and to obtain satisfactory stent expansion, additional dilatation plus the original radial force of a self-expanding stent seems essential through postdi-

lation with a balloon catheter. However, hypotension and bradycardia from the stretching of the carotid sinus baroreceptor after CAS are known to be influenced by the magnitude of the dilation performed,<sup>23</sup> and moreover, several reports<sup>10,11</sup> also indicated that the presence of calcification in plaque was significantly related with increased rate of stent fracture or deformation. Expansion of the stent was therefore occasionally reduced, especially in severe carotid stenosis. We calculated the improvement rate of stenosis in the present study. The mean improvement rate of the HCP group was, however, lower than that of the LCP group after CAS ( $87.0\% \pm 16.8\%$  v  $97.9\% \pm 7.9\%$ ), whereas CEA had good improvement rates regardless of calcification in plaques.

The reason that residual stenosis after CAS for the LCP group was even less than that of the CEA group in our study is not apparent. The percentage using the Wallstent was not significantly different (18.8% for HCP and 14.0% for LCP), and the same balloon catheters were used for both groups. We strictly counted transient dents made by tourniquets used in CEA as residual stenosis that could be usually restored in a year, which might lead to a relatively higher degree of residual stenosis in CEA.

It was reported in 2008 that the total volume of calcification in carotid plaques did not correlate with residual stenosis,<sup>24</sup> and the study's authors concluded that CAS using embolic protection devices was feasible even in patients with near-total circumferential plaque calcification. They also reported that fragmentations of the calcifications were confirmed in 17 of 18 plaques with a mean arc of calcification ranging from 278° to 360°.<sup>25</sup> However, in these studies, the plaque calcification volume was determined by manual tracing on computed tomographic sections, without an assessment of the hardness of the calcification, and the results were not compared with those after CEA. From the results of the present study, it might be important to analyze calcified plaques using calcium scores for precise assessment of calcification

**Figure 3.** A right carotid artery stenting case of a 77-year-old man with 90% carotid stenosis. (A) Preoperative computed tomography angiography (CTA) revealed a high-calcified plaque at the right carotid bifurcation (calcium score 1076.8). (B) Carotid artery stenting was performed using a PRECISE stent (Cordis, Bridgewater, NJ) with predilatation (6 atm, 30 sec) and postdilatation (10 atm, 15 sec) by balloon catheters and a PercuSurge Guardwire (Medtronic, Santa Rosa, CA) distal balloon embolic protection device. Postoperative CTA revealed calcification outside the stent, as it was preoperatively. (C) A sagittal multiplanar reconstruction image of the postoperative CTA scan revealed 27.6% residual stenosis with calcification outside the stent (arrowheads). (D) An axial multiplanar reconstruction image of the postoperative CTA scan also revealed restriction in the stent expansion from calcification (arrowheads).



- of several anti-embolic protection devices. *Neurol Med Chir (Tokyo)* 2009;49:386-393.
5. Katano H, Kato K, Umemura A, et al. Perioperative evaluation of carotid endarterectomy by 3D-CT angiography with refined reconstruction: Preliminary experience of CEA without conventional angiography. *Br J Neurosurg* 2004;18:138-148.
  6. Niwa Y, Katano H, Yamada K. Calcification in carotid atheromatous plaque: Delineation by 3D-CT angiography, compared with pathological findings. *Neurol Res* 2004; 26:778-784.
  7. Katano H, Yamada K. Analysis of calcium in carotid plaques with Agatston scores for appropriate selection of surgical intervention. *Stroke* 2007;38:3040-3044.
  8. Nonaka T, Oka S, Miyata K, et al. Prediction of prolonged postprocedural hypotension after carotid artery stenting. *Neurosurgery* 2005;57:472-477.
  9. Tyden G, Samnegard H, Thulin L. Rational treatment of hypotension after carotid endarterectomy by carotid sinus nerve blockade. *Acta Chir Scand Suppl* 1980; 500:61-64.
  10. Chang CK, Huded CP, Nolan BW, et al. Prevalence and clinical significance of stent fracture and deformation following carotid artery stenting. *J Vasc Surg* 2011; 54:685-690.
  11. Coppi G, Moratto R, Veronesi J, et al. Carotid artery stent fracture identification and clinical relevance. *J Vasc Surg* 2010;51:1397-1405.
  12. North American Symptomatic Carotid Endarterectomy Trial Collaborators. Beneficial effect of carotid endarterectomy in symptomatic patients with high-grade carotid stenosis. *N Engl J Med* 1991;325:445-453.
  13. Executive Committee for the Asymptomatic Carotid Atherosclerosis Study. Endarterectomy for asymptomatic carotid artery stenosis. *JAMA* 1993;273:1421-1428.
  14. Yadav JS, Wholey MH, Kunts RE, et al. Stenting and angioplasty with protection in patients at high risk for endarterectomy investigators. Protected carotid-artery stenting versus endarterectomy in high-risk patients. *N Engl J Med* 2004;351:1453-1501.
  15. Brott TG, Hobson RW II, Howard G, et al. Stenting versus endarterectomy for treatment of carotid-artery stenosis. *N Engl J Med* 2010;363:11-23.
  16. Katano H, Yamada K. Carotid endarterectomy for stenoses of twisted carotid bifurcations. *World Neurosurgery* 2010;73:147-154.
  17. Hosoda K, Kawaguchi T, Ishii K, et al. Comparison of conventional region of interest and statistical mapping method in brain single-photon emission computed tomography for prediction of hyperperfusion after carotid endarterectomy. *Neurosurgery* 2005;57:32-41.
  18. Takeuchi R, Sengoku T, Matsumura K. Usefulness of fully automated constant ROI analysis software for the brain: 3DSRT and FineSRT. *Radiat Med* 2006;24:538-544.
  19. Torigai T, Mase M, Ohno T, et al. Usefulness of dual and fully automated measurements of cerebral blood flow during balloon occlusion test of the internal carotid artery. *J Stroke Cerebrovasc Dis* 2011 September 17 [Epub ahead of print].
  20. McCabe DJH, Pereira AC, Clifton A, et al. Restenosis after carotid angioplasty, stenting, or endarterectomy in the Carotid and Vertebral Artery Transluminal Angioplasty Study (CAVATAS). *Stroke* 2005;36:281-286.
  21. Aronow HD, Gray WA, Ramee SR, et al. Predictors of neurological events associated with carotid artery stenting in high-surgical-risk patients. Insights from the Cordis Carotid Stent Collaborative. *Circ Cardiovasc Interv* 2010;3:577-584.
  22. Randall MS, McKeivitt FM, Kumar S, et al. Long-term results of carotid artery stents to manage symptomatic carotid artery stenosis and factors that affect outcome. *Circ Cardiovasc Interv* 2010;3:50-56.
  23. Lavoie P, Rutledge J, Dawoud MA, et al. Predictors and timing of hypotension and bradycardia after carotid artery stenting. *AJNR Am J Neuroradiol* 2008;29:1942-1947.
  24. Tsutsumi M, Aikawa H, Onizuka M, et al. Carotid artery stenting for calcified lesions. *AJNR Am J Neuroradiol* 2008;29:1590-1593.
  25. Tsutsumi M, Kodama T, Aikawa H, et al. Fragmentation of calcified plaque after carotid artery stenting in heavily calcified circumferential stenosis. *Neuroradiology* 2010; 52:831-836.
  26. Schnaudigel S, Gröschel K, Pilgram SM, et al. New brain lesions after carotid stenting versus carotid endarterectomy. A systematic review of the literature. *Stroke* 2008; 39:1911-1919.
  27. Watarai H, Kaku Y, Yamada M, et al. Follow-up study on in-stent thrombosis after carotid stenting using multidetector CT angiography. *Neuroradiology* 2009;51:243-251.
  28. Mas JL, Chatellier G, Beyssen B. Carotid angioplasty and stenting with and without cerebral protection: Clinical alert from the Endarterectomy Versus Angioplasty in Patients With Symptomatic Severe Carotid Stenosis (EVA-3S) trial. *Stroke* 2004;35:e18-e21.
  29. Goodney PP, Nolan BW, Eldrup-Jorgensen J, et al. Vascular study group of Northern New England: Restenosis after carotid endarterectomy in a multicenter regional registry. *J Vasc Surg* 2010;52:897-905.
  30. Hellings WE, Moll FL, De Vries JP, et al. Atherosclerotic plaque composition and occurrence of restenosis after carotid endarterectomy. *JAMA* 2008;299:547-554.
  31. Makihara N, Toyoda K, Uda K, et al. Characteristic sonographic findings of early restenosis after carotid endarterectomy. *J Ultrasound Med* 2008;27:1345-1352.
  32. Mannheim D, Weller B, Vahadim E, et al. Carotid endarterectomy with a polyurethane patch versus primary closure: A prospective randomized study. *J Vasc Surg* 2005; 41:403-408.
  33. Kaku Y, Yoshimura S, Kokuzawa J. Factors predictive of cerebral hyperperfusion after carotid angioplasty and stent placement. *AJNR Am J Neuroradiol* 2004; 25:1403-1408.
  34. van Mook WNKA, Rennenberg RJMW, Schurink GW, et al. Cerebral hyperperfusion syndrome. *Lancet Neurol* 2005;4:877-888.
  35. Arquizán C, Trinquart L, Touboul PJ, et al. Restenosis is more frequent after carotid stenting than after endarterectomy: The EVA-3S Study. *Stroke* 2011;42:1015-1020.

# Protection by Physical Activity Against Deleterious Effect of Smoking on Carotid Intima-media Thickness in Young Japanese

Hiroyuki Katano, MD,\*† Masahiro Ohno, MD,‡ and Kazuo Yamada, MD\*

**Background:** The hazardous effects of smoking and the favorable influence of physical activity on the progression of atherosclerosis have been well studied, but little is known about the interactions of these 2 factors. **Methods:** A total of 1090 subjects who were screened for brain disease (at annual medical checkups) between April 2007 and March 2008 were studied to clarify the effects of smoking on maximum carotid intima-media thickness (IMT) in patients with different grades of physical activity. Univariate and multivariate analyses were performed to investigate relationships between maximum IMT and independent variables, such as smoking status, age, gender, coexisting disease, physical activity, alcohol drinking, family history, subjective symptoms, body mass index, systolic blood pressure, diastolic blood pressure, blood sugar, total cholesterol, high-density lipoprotein cholesterol, and triglycerides. **Results:** Univariate analysis revealed only the low physical activity group to have a significant relationship between smoking and maximum IMT. When the subjects were divided into 3 age groups ( $\leq 49$ , 50-59, and  $\leq 60$  years of age, respectively), the same association was noted for high and moderate physical activity groups  $\leq 49$  years of age. Multivariate analysis further revealed smoking status to be a significant predictor of maximum IMT in the young low and moderate activity groups. **Conclusions:** In physically inactive young people, smoking might have detrimental effects on maximum IMT, while high physical activity may be protective. **Key Words:** Carotid artery—intima-media thickness—physical activity—smoking.

© 2011 by National Stroke Association

Smoking has hazardous effects on health. Cigarette smoking increases the risk of cerebrovascular and cardiovascular events and is well documented to be a risk factor for ischemic stroke in general, with relative risks of 1.5 to 5.7.<sup>1</sup> It has also been reported that smoking increases carotid intima-media thickness (IMT),<sup>2</sup> which is a well-known surrogate marker for atherosclerosis.<sup>3</sup>

In contrast, appropriate physical activity may promote health, reducing cardiovascular and cerebrovascular events, while inactivity may increase risk of stroke,<sup>4</sup> although the issue is still controversial.<sup>5-7</sup> Concerning physical activity and IMT, most reports have revealed a reverse association, but the data are inconclusive.<sup>8-10</sup>

Few investigators, however, have analyzed the relationship between the effects of smoking and physical activity in detail.<sup>4,5,11</sup> We investigated a series of Japanese patients undergoing a brain dock, an annual physical check for cerebral disease, to clarify the effects of smoking on people with different grades of physical activity. We used maximum IMT of the carotid artery on carotid ultrasonography as the end point.

## Methods

### Subjects

A total of 2012 subjects (1369 men and 643 women 54.3  $\pm$  9.6 years of age) visited the Health Management

From the \*Departments of Neurosurgery; †Medical Informatics and Integrative Medicine, Nagoya City University Graduate School of Medical Sciences; and ‡Health Management Center, Chunchi Hospital, Nagoya, Japan.

Received June 12, 2011; accepted July 14, 2011.

Address correspondence to: Hiroyuki Katano, MD, Department of Neurosurgery, Nagoya City University Graduate School of Medical Sciences, 1 Kawasumi, Mizuho-cho, Mizuho-ku, Nagoya 467-8601, Japan. E-mail: katano@med.nagoya-cu.ac.jp.

1052-3057/\$ - see front matter

© 2011 by National Stroke Association

doi:10.1016/j.jstrokecerebrovasdis.2011.07.009

**Results**

The 1090 patients included 756 males and 334 females. Their clinical characteristics are summarized in Table 1. Average ages of the high physical activity group were rather higher than with the moderate and low physical activity groups ( $P = .0002$  and  $P < .0001$ , respectively). This may be because of greater numbers of health conscious people in the middle- and high-age groups. Systolic blood pressure was higher in the high physical activity group ( $P = .026$  and  $P = .095$ , respectively). No significant differences were detected for other continuous variables. Mean values for maximum IMT were higher in the high physical activity group than in the moderate and low physical activity groups (both  $P < .0001$ ). The relatively high average age of patients in the high physical activity group described above may have the relation to it.

Differences in maximum IMT among 3 groups of smoking status in each physical activity group were analyzed by multigroup analyses (Table 2). In high and moderate physical activity groups, no significant differences in maximum IMT were found among 3 smoking status groups, whereas with low physical activity, significant differences were found between current and never smokers ( $P = .003$ ) and former and never smokers ( $P = .025$ ).

Univariate analysis also revealed a significant association between smoking status and maximum IMT for the low physical activity group ( $\rho = 0.182$ ;  $P < .0001$ ; Table 3).

Given the age-dependence observed, univariate analysis was reconduted with division into 3 age subgroups ( $\leq 49$ , 50-59, and  $\leq 60$  years old; Table 4). With low physical activity, smoking had significant associations with maximum IMT in all 3 groups ( $\rho = 0.159$  and  $P = .026$ ,  $\rho = 0.169$  and  $P = .006$ , and  $\rho = 0.169$  and  $P = .050$ , respectively). This was also the case for high and moderate physical activity groups  $\leq 49$  years of age ( $\rho = 0.293$  and  $P = .031$ ;  $\rho = 0.268$  and  $P = .041$ , respectively).

Results of multivariate analysis for different physical activity in each age group for the 9 independent variables are summarized in Table 5. With  $R^2$  analyses, smoking status was a significant predictor for maximum IMT in young moderate and low physical activity groups ( $F = 7.343$  and  $P = .009$ ;  $F = 3.929$  and  $P = .049$ , respectively). Smoking status in patients  $\geq 60$  years of age high and low physical activity groups had  $P$  values for  $F$  statistics  $< .05$ , but the  $R^2$  values were low.

**Discussion**

The present study provides evidence of smoking and physical activity interactions with regard to the maximum IMT endpoint in the youngest age group. In the group  $\leq 49$  years of age amelioration of the detrimental effects of smoking may be observed with high levels of exercise. Regarding smoking alone, our results are in line with the literature. Love et al<sup>12</sup> inspected young adults

**Table 1.** Mean values for factor with reference to intensity of physical activity

	Total (n = 1090)	P value*	High physical activity (n = 303)	Moderate physical activity (n = 191)	Low physical activity (n = 596)	P value† (versus high)
Current smoker (%)	252	—	48 (15.8)	40 (20.9)	164 (27.5)	—
Former smoker (%)	245	—	92 (30.4)	42 (22.0)	111 (18.6)	—
Never smoker (%)	593	—	163 (53.8)	109 (57.1)	321 (53.9)	—
Male (%)	756 (69.4)	.077	225 (74.3)	125 (65.4)	407 (68.3)	—
Age, y	54.1 ± 9.9	<.0001*	57.7 ± 9.7	54.5 ± 8.5	53.3 ± 9.2	<.0001
Body mass index, kg/m <sup>2</sup>	23.5 ± 9.1	.071	24.3 ± 16.5	22.7 ± 3.4	23.3 ± 3.3	—
Systolic blood pressure, mm Hg	114.4 ± 37.6	.023*	118.2 ± 65.6	110.4 ± 16.4	113.8 ± 17.7	.095
Diastolic blood pressure, mm Hg	69.6 ± 13.1	.185	69.9 ± 13.0	68.5 ± 13.2	69.7 ± 13.1	—
Blood sugar, mg/dL	102.3 ± 18.4	.499	102.8 ± 19.4	101.2 ± 13.1	102.4 ± 19.3	—
Total cholesterol, mg/dL	206.4 ± 35.0	.521	208.4 ± 32.6	207.3 ± 36.1	205.2 ± 35.9	—
HDL cholesterol, mg/dL	60.2 ± 15.2	.094	62.0 ± 16.1	60.4 ± 15.1	59.3 ± 14.7	—
Triglycerides, mg/dL	120.1 ± 84.3	.084	116.1 ± 73.9	113.7 ± 90.1	124.2 ± 87.3	—
Maximum IMT, mm	1.04 ± 0.72	<.0001*	1.18 ± 0.78	1.11 ± 0.83	1.02 ± 0.77	<.0001

Abbreviations: HDL, high-density lipoprotein; IMT, intima-media thickness.

Plus/minus values are means ± standard deviation or number of subjects (for gender).

\*Kruskal-Wallis test.

†Bonferroni/Dunn post hoc test (versus high physical activity).

**Table 4.** Age-specific univariate analysis of maximum intima-media thickness with each factor for 3 intensities of physical activity

Age, y	≤49		50-59		≥60	
	$\rho$	<i>P</i>	$\rho$	<i>P</i>	$\rho$	<i>P</i>
High physical activity	n = 55		n = 125		n = 123	
Smoking status	0.293*	.031	-0.027	.767	0.112	.215
Age	0.119	.382	0.194	.031	0.240	.008
Coexisting disease	0.410	.003	0.022	.809	0.246	.007
Alcohol drinking	-0.006	.965	0.226	.012	-0.126	.164
Family history	0.276	.043	0.007	.940	-0.012	.896
Subjective symptom	-0.044	.747	-0.113	.208	-0.096	.290
Body mass index	0.255	.061	0.014	.879	-0.057	.531
Systolic blood pressure	0.173	.205	0.171	.058	0.010	.909
Diastolic blood pressure	0.319	.019	0.095	.290	-0.152	.093
Blood sugar	0.316	.020	0.029	.745	0.075	.679
Total cholesterol	-0.064	.638	-0.001	.993	0.037	.278
HDL cholesterol	-0.327	.016	-0.096	.283	-0.098	.818
Triglycerides	0.267	.050	0.120	.183	-0.021	.717
Male sex†	—	.039	—	.006	-0.033	.390
Moderate physical activity	n = 59		n = 73		n = 59	
Smoking status	0.268*	.041	-0.145	.219	0.124	.345
Age	0.372	.005	0.141	.230	0.231	.079
Coexisting disease	0.104	.430	0.289	.014	0.156	.235
Alcohol drinking	0.072	.585	-0.116	.323	-0.086	.512
Family history	-0.050	.702	-0.093	.400	0.170	.196
Subjective symptom	0.139	.291	-0.032	.430	-0.067	.610
Body mass index	0.354	.007	-0.027	.818	0.054	.682
Systolic blood pressure	0.271	.039	0.178	.131	0.274	.037
Diastolic blood pressure	0.223	.090	0.217	.066	0.141	.285
Blood sugar	0.195	.137	0.042	.721	0.006	.963
Total cholesterol	0.444	.001	0.026	.826	-0.034	.794
HDL cholesterol	-0.130	.324	-0.080	.500	0.053	.688
Triglycerides	0.389	.003	-0.092	.434	-0.083	.525
Male sex†	—	.236	—	.169	—	.405
Low physical activity	n = 198		n = 262		n = 136	
Smoking status	0.159*	.026	0.169*	.006	0.169*	.050
Age	0.264	.000	0.165	.008	0.162	.060
Coexisting disease	0.148	.038	0.230	.000	0.206	.017
Alcohol drinking	0.116	.105	0.127	.040	0.107	.214
Family history	0.298	.766	0.022	.719	-0.019	.825
Subjective symptom	-0.056	.429	-0.094	.130	0.062	.469
Body mass index	0.161	.024	0.143	.021	-0.025	.768
Systolic blood pressure	0.144	.043	0.238	.000	0.069	.720
Diastolic blood pressure	0.218	.002	0.179	.004	-0.028	.745
Blood sugar	0.205	.004	0.117	.059	0.093	.279
Total cholesterol	0.173	.015	-0.044	.474	-0.059	.491
HDL cholesterol	-0.227	.002	-0.225	.000	0.029	.737
Triglycerides	0.286	<.0001	0.170	.006	0.070	.944
Male sex†	—	.000	—	.006	—	.002

Abbreviation: HDL, high-density lipoprotein.

\*Spearman correlation test.

†Mann-Whitney analysis.

activity in women and men to be associated with an increased risk of stroke (relative risk 1.83%).

On the other hand, Evenson et al<sup>5</sup> investigated 14,575 individuals followed for an average of 7.2 years and showed that physical activity was only weakly associated

with ischemic stroke risk. In the Framingham study, among an older cohort, the strongest protective effect was detected in the medium tertile physical activity subgroup, with no additional benefit gained from higher levels of physical activity. Lee et al<sup>6</sup> reported the results

of a prospective cohort study of 11,130 Harvard University alumni, revealing that with higher levels of energy expenditure (up to 3000 kcal/week), risk declined steadily, but beyond this the association weakened. Walking >20 km per week was associated with significantly lower risk, while light intensity activities (<4.5 metabolic equivalent tasks) were unrelated. Wannamethee and Shaper<sup>7</sup> pointed out that the benefit of vigorous physical activity for stroke was offset by an increased risk of heart attack.

In most previous studies, interactions between physical activity and smoking were not of major concern.<sup>5</sup> Sacco et al<sup>4</sup> stated briefly that the protective effects of physical activity did not differ by smoking status, unlike other risk factors, such as hypertension, diabetes, and cardiac disease. Gillum et al<sup>11</sup> speculated that high nonrecreational physical activity was less protective in white male smokers than in nonsmokers, but did not provide detailed data to this end. The Honolulu Heart Program, covering only older middle-aged men of Japanese ancestry, revealed a protective effect of habitual physical activity against thromboembolic stroke that was limited to their nonsmoking group.<sup>22</sup>

Here, we found smoking status to be a significant prediction was noted of maximum IMT in all age groups with low physical activity. Even with high and moderate physical activity, significant prediction was noted in patients  $\leq 49$  years of age.

Concerning people in the same age group with high physical activity, however, smoking status was not selected as a predictor of maximum IMT with multivariate analysis ( $F = 3.501$ ;  $P = .068$ ). There are 2 plausible interpretations for these results. One is the attenuation of hazardous effects of smoking by the beneficial effects of physical activity, and the other is that other independent factors are more influential determinants. With older age groups, the fact that thickening of intima and atherosclerosis occur because of many factors as people age<sup>23</sup> may result in attenuation of the malicious effects of smoking as a whole.

There are limitations to the present study. First, although the subjects were randomly selected independent of the present study purpose during each week of the study period, there is still a possibility of selection bias. Second, because carotid IMT measurement was made using ultrasonographic methods, inter- and intraobserver variability is conceivable, although all 3 examiners were experienced. Third, physical activities were classified into 3 groups according to the intensity of activity but were not quantitatively determined—for example, using a minimum equivalent task score or the International Physical Activity Questionnaire.<sup>24,25</sup> Fourth, medications such as statins,<sup>26</sup> antihypertensives,<sup>27</sup> and antiplatelets,<sup>28</sup> which are reported to decrease IMT (mostly mean IMT), were not considered. Finally, we did not control for environmental smoke exposure in nonsmokers, which has

been reported to increase the risk of cardiovascular and cerebrovascular events.<sup>29-31</sup>

The present study shows that at least in young people ( $\leq 49$  years of age), physically inactive smokers tend to have a higher maximum IMT. There is a possibility that in this age group, the detrimental effects of smoking on maximum IMT may be alleviated by physical activity.

## References

1. You B, McNeil JJ, O'Malley HM, et al. Risk factors for lacunar infarction syndromes. *Neurology* 1995;45:1483-1487.
2. Tell GS, Howard G, McKinney WM, et al. Cigarette smoking cessation and extracranial carotid atherosclerosis. *JAMA* 1989;261:1178-1180.
3. O'Leary DH, Polak JF, Kronmal RA, et al. Cardiovascular Health Study Collaborative Research Group. Carotid-artery intima and media thickness as a risk factor for myocardial infarction and stroke in older adults. *N Engl J Med* 1999;340:14-22.
4. Sacco RL, Gan R, Boden-Albala B, et al. Leisure-time physical activity and ischemic stroke risk: The Northern Manhattan Stroke Study. *Stroke* 1998;29:380-387.
5. Evenson KR, Rosamond WD, Cai J, et al. Physical activity and ischemic stroke risk: The Atherosclerosis Risk in Communities Study. *Stroke* 1999;30:1333-1339.
6. Lee I-M, Paffenbarger RS Jr. Physical activity and stroke incidence: The Harvard Alumni Health Study. *Stroke* 1998;29:2049-2054.
7. Wannamethee G, Shaper AG. Physical activity and stroke in British middle aged men. *BMJ* 1992;304:597-601.
8. Elbaz A, Ripert M, Tavernier B, et al. Common carotid artery intima-media thickness, carotid plaques, and walking speed. *Stroke* 2005;36:2198-2202.
9. Kadoglou NP, Iliadis F, Liapis CD. Exercise and carotid atherosclerosis. *Eur J Vasc Endovasc Surg* 2008;35:264-272.
10. Sato S, Makita S, Uchida R, et al. Physical activity and progression of carotid intima-media thickness in patients with coronary heart disease. *J Cardiol* 2008;51:157-162.
11. Gillum RF, Mussolino ME, Ingram DD. Physical activity and stroke incidence in women and men. *Am J Epidemiol* 1996;143:860-869.
12. Love BB, Biller J, Jones MP, et al. Cigarette smoking. A risk factor for cerebral infarction in young adults. *Arch Neurol* 1990;47:693-698.
13. Robbins AS, Manson JE, Lee IM, et al. Cigarette smoking and stroke in a cohort of US male physicians. *Ann Intern Med* 1994;120:458-462.
14. Bhat VM, Cole JW, Sorkin JD, et al. Dose-response relationship between cigarette smoking and risk of ischemic stroke in young women. *Stroke* 2008;39:2439-2443.
15. Mast H, Thompson JLP, Lin I-F, et al. Cigarette smoking as a determinant of high-grade carotid artery stenosis in Hispanic, black, and white patients with stroke of transient ischemic attack. *Stroke* 1998;29:908-912.
16. Nakashima A, Yorioka N, Asakimori Y, et al. Different risk factors for the maximum and the mean carotid intima-media thickness in hemodialysis patients. *Intern Med* 2003;42:1095-1099.
17. Adachi H, Hirai Y, Fujiura Y, et al. Plasma homocysteine levels and atherosclerosis in Japan: Epidemiological study by use of carotid ultrasonography. *Stroke* 2002;33:2177-2181.

Original Paper

## Plaque Vulnerability in Internal Carotid Arteries with Positive Remodeling

Toshiyasu Miura<sup>a</sup> Noriyuki Matsukawa<sup>a</sup> Keita Sakurai<sup>b</sup>  
Hiroyuki Katano<sup>c</sup> Yoshino Ueki<sup>a</sup> Kenji Okita<sup>a</sup> Kazuo Yamada<sup>c</sup>  
Kosei Ojika<sup>a</sup>

Departments of <sup>a</sup>Neurology, <sup>b</sup>Radiology and <sup>c</sup>Neurosurgery, Nagoya City University, Nagoya, Japan

### Key Words

Black-blood magnetic resonance image · Carotid artery · Multidetector-row computer tomography · Plaque vulnerability · Positive remodeling

### Abstract

**Background:** This study aimed to evaluate the efficacy of assessing positive remodeling for predicting future stroke events in the internal carotid artery. We therefore assessed narrowing of the carotid artery lumen using multidetector-row computer tomography (MDCT) angiography and carotid plaque characteristics using black-blood (BB) magnetic resonance (MR). **Methods:** We retrospectively selected 17 symptomatic and 11 asymptomatic lesions with luminal narrowing >50%. We compared remodeling parameters of luminal stenosis (remodeling ratio, RR/remodeling index, RI) using MDCT and MR intensities of atherosclerotic plaque contents using the BB technique (relative signal intensity, rSI). We also confirmed the validity of the relationship between MR intensity and atherosclerotic plaque contents by histology. The levels of biological markers related to vessel atherosclerosis were measured. **Results:** Plaque lesions with positive remodeling in carotid arteries were associated with a significantly higher prevalence of stroke compared with plaques with negative remodeling ( $p < 0.05$ ). Radiologic and histologic analyses determined that plaques with positive remodeling had higher signal intensities (with respect to their lipid-rich content or to hemorrhage) compared with negative remodeling (correlation coefficients: RI and rSI,  $r = 0.41$ ,  $p < 0.05$ ; RR and rSI,  $r = 0.50$ ,  $p < 0.05$ ). Levels of biological markers, including high-sensitivity C-reactive protein, hemoglobin A1C, total cholesterol, low-density lipoprotein cholesterol and high-density lipoprotein cholesterol, were not useful for predicting stroke events. **Conclusions:** The results of this study suggest that the combined analysis of RR, RI and rSI could potentially help to predict future stroke events.

Copyright © 2011 S. Karger AG, Basel

## Introduction

The formation of atherosclerotic plaques in the extracranial internal carotid arteries is a common cause of cerebrovascular disease. Carotid endarterectomy (CEA) and carotid arterial stenting (CAS) can be useful interventions for preventing secondary strokes in patients unresponsive to medical therapy. The decision to perform interventional therapies is currently based on the percent luminal narrowing of the vessel [1–3]. However, some patients with minimal stenosis in extracranial internal carotid arteries can unexpectedly experience strokes related to the rupture of atherosclerotic plaques, whereas other patients with severe stenosis remain stroke free. Better methods of distinguishing between these patients are needed to decide on the optimal treatment, i.e. CEA or CAS, versus medical therapy.

Several recent studies have indicated that coronary arteries may respond to plaque growth in two different ways: either by outward expansion of the vessel wall (positive remodeling) or by vessel shrinkage (negative remodeling) [4]. In coronary events, positive remodeling may be associated with an unstable clinical presentation, whereas negative remodeling may be more common in patients with stable clinical presentations [5]. Coronary artery plaques with positive remodeling have also been shown histologically to have a higher lipid content and macrophage count [6]. The vulnerability of an atherosclerotic plaque to rupture is considered to be related to its intrinsic composition, including the size of the lipid core and the presence of intraplaque hemorrhage [7]. Indeed, the characteristics of atherosclerotic plaques were shown to strongly correlate with the prevalence of coronary events in patients with coronary stenosis caused by atherosclerotic plaques [8].

A previous report suggested that the extent of expansive remodeling may also indicate underlying atherosclerotic plaque vulnerability in internal carotid artery stenosis [9]. This report assessed the remodeling ratio (RR, i.e. the ratio of outside vessel circumference between the point of maximal luminal stenosis and the unaffected region) and investigated the correlation between this ratio and the prevalence of stroke. However, the role of the qualitative histologic characteristics of carotid artery atherosclerotic plaques in plaque vulnerability remains unknown.

Multidetector-row computer tomography (MDCT) angiography is a powerful, noninvasive tool for rapidly assessing the percent luminal narrowing in carotid arteries. Although it may be inferior to magnetic resonance imaging (MRI) for determining the histologic characteristics of plaques, MDCT has been reported to be able to differentiate between internal plaque components [10].

However, the combination of spin echo-based  $T_1$ -,  $T_2$ - and intermediate-weighted imaging and of  $T_2^*$ -weighted gradient recall echo in MRI was reported to be useful for evaluating individual histologic plaque components [11, 12]. Recent studies demonstrated the use of pulse sequences designed for vascular imaging, namely black-blood (BB) techniques [13, 14]. However, these BB techniques are based on the acquisition of two-dimensional data with a section thickness of 2–5 mm, making it difficult to capture the whole picture and determine the maximal percent luminal narrowing in carotid arteries.

This study aimed to elucidate the association between carotid artery positive remodeling and the risk of incident stroke using a combination of MDCT angiography and noninvasive MR characterization. We confirmed that histologic classification by MRI matched plaque characterization. We designed a retrospective study to assess carotid artery luminal narrowing using MDCT angiography and carotid plaque characteristics using the BB MR technique. The reliability of the results was confirmed by direct comparison of some carotid plaques obtained by CEA with the results of BB MRI.

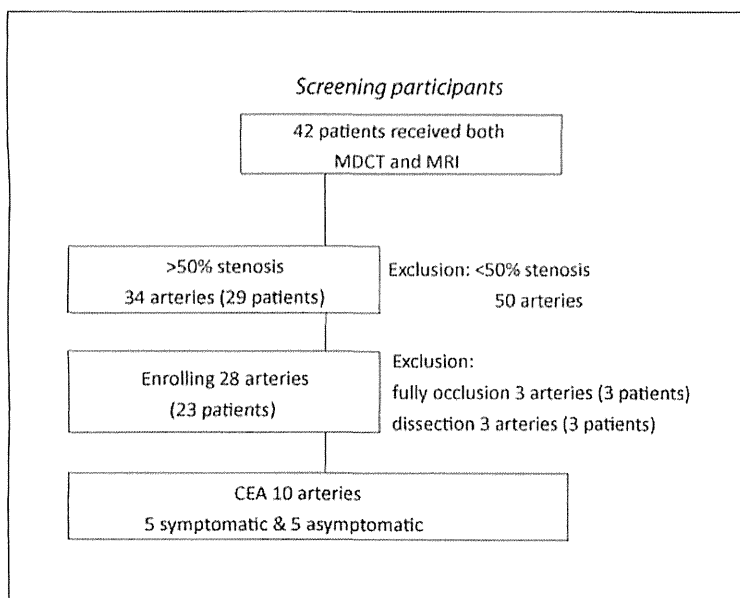


**Fig. 1.** Patient screening. Forty-two participants who underwent both MDCT angiography and BB MR analysis were identified in the Nagoya City University Medical Center database from August 2008 to July 2010; 50 arteries were excluded because of stenosis <50% in NASCET, and 6 arteries were excluded because of the presence of other potential causes of neurologic symptoms (full occlusion, 3 arteries, and possible dissection, 3 arteries). Twenty-eight arteries were finally enrolled in this study; 10 of the 28 were treated surgically (CEA).

## Subjects and Methods

This study was approved by the Medical Ethics Committee of the Nagoya City University Graduate School of Medical Sciences. Informed patient consent was not required.

### *Patient Population*

The study group was selected following a search of the patient database of the Nagoya City University Medical Center from August 2008 to July 2010. Patient backgrounds were standardized by applying the following inclusion criteria: (1) received both dedicated MDCT angiography and BB MR analysis of the neck using the same imaging parameters, and (2) neuroradiologic verification by a neurologist. During this period, a total of 84 carotid arteries (42 patients) received both MDCT angiography and analysis of plaque characteristics by BB MR. Of these 84 carotid arteries, 34 (29 patients) demonstrated >50% atherosclerotic stenosis. Six carotid arteries (6 patients) were excluded from the study because of the presence of other potential causes for their neurologic symptoms (full occlusion, 3 arteries, and possible dissection, 3 arteries). Twenty-three Japanese patients (all males, mean age  $70.6 \pm 6.5$  years) with a total of 28 lesions were finally enrolled in this study (fig. 1).

### *Definitions of Symptomatic and Asymptomatic Patients*

Enrolled patients were classified to have either (1) a symptomatic lesion with a documented neurologic event (stroke, transient ischemic attack or amaurosis fugax) in a vascular distribution concordant with the affected carotid artery, or (2) an asymptomatic atherosclerotic lesion. Transient ischemic attack and stroke events were defined on the basis of previ-

**Table 1.** Baseline patient demographics and clinical characteristics (means  $\pm$  SD)

Variables	Symptomatic	Asymptomatic	p value
Lesions, n	17	11	
Age, years	71.1 $\pm$ 1.1	70.6 $\pm$ 7.8	>0.05
NASCET, %	77.5 $\pm$ 14.5	70.6 $\pm$ 10.0	>0.05
Risk factors			
Hypertension	13	8	>0.05
Dyslipidemia	13	7	>0.05
Diabetes	9	7	>0.05
Smoking	6	5	>0.05

ously published criteria [15, 16]. Amaurosis fugax was defined as acute onset of transient complete or partial monocular loss of vision. The final 28 lesions included 17 symptomatic and 11 asymptomatic lesions (table 1).

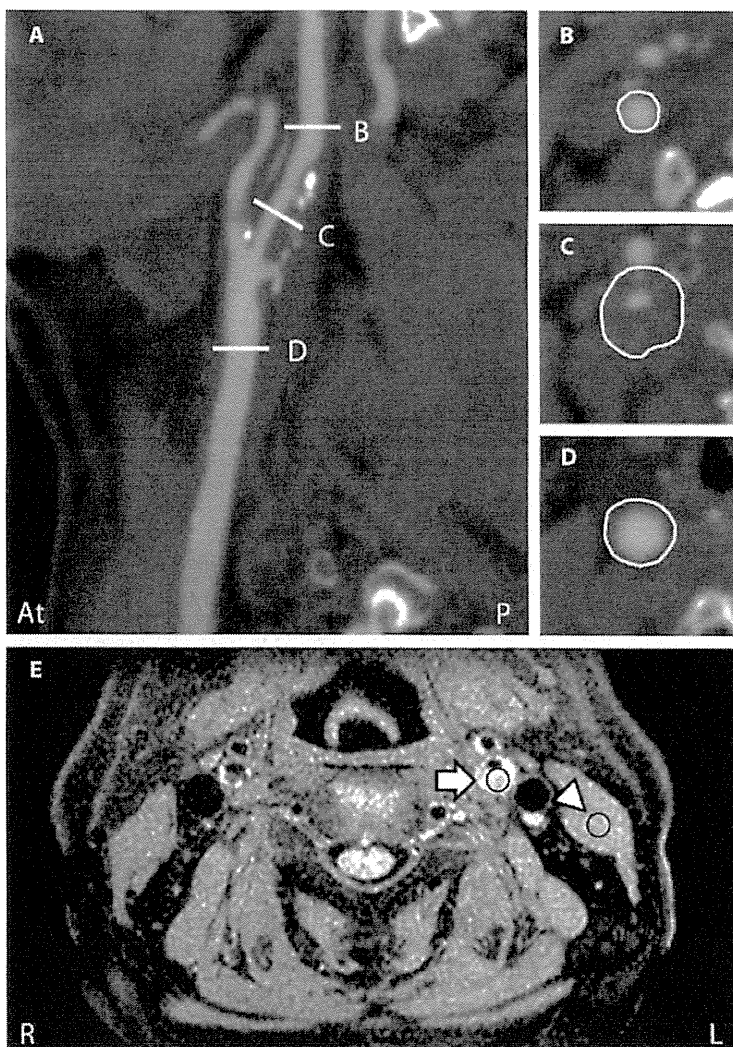
#### Computed Tomography

MDCT angiography was performed in all study patients using helical acquisition with a 64-detector row CT scanner (SOMATOM Definition; Siemens Medical Solutions, Forchheim, Germany) with two X-ray tubes mounted onto a single gantry at an angle of 90°. The imaging acquisition parameters were as follows: spiral mode 0.33-second gantry rotation; collimation, 32  $\times$  0.6 mm; pitch factor, 1.5; section thickness 1.0 mm; reconstruction interval, 0.5 mm, and acquisition parameters 120 kVp and 350 mA. A total 50 ml of non-ionized contrast medium, iohexol (Omnipaque 300; Dainichi Sankyo, Tokyo, Japan) or iopamidol (Iopamiron 300; Bayer Schering Pharma, Berlin, Germany), was injected at a flow rate of 3.5 ml/s, followed by 25 ml of a saline chaser at the same rate as the contrast medium. Optimal timing of MDCT angiography acquisition was determined by an automated bolus-timing program. Images were obtained from the aortic arch to the level of the inferior orbits. The image data were transferred to a computer workstation (Ziostation version 1.17; Amin, Tokyo, Japan) for image post-processing.

#### Image Analysis

All measurements of luminal stenosis were performed by a single experienced neuroradiologist (K.S.) who was blinded to the clinical information. The degree of luminal stenosis in the carotid arteries was evaluated by image analysis of an axial image and curved multiplanar reconstruction to produce a two-dimensional image showing the cross-sectional profile of a vessel along its length [1] (fig. 2A, C). The degree of stenosis was determined by the neuroradiologist on the basis of these data, following the criteria of the North American Symptomatic Carotid Endarterectomy Trial (NASCET). After identifying the atherosclerotic lesions on axial images, serial cross-sectional images of the carotid arteries were obtained by changing the orientation of the z-axis to analyze the proximal portions of the internal carotid arteries. Using image display settings of window level 250 and width 700, the region of maximum luminal narrowing was visually identified and the outer vessel contour was manually traced to allow calculation of the cross-sectional vessel area (CSA; fig. 2C). In addition, reference CSAs were measured at the nearest proximal and distal segments without atherosclerotic plaques, and the mean values of these were calculated as reference CSAs (fig. 2B, D). On the basis of these numerical values, two values were calculated to assess plaque remodeling of carotid arteries: the plaque remodeling index (RI), which was calcu-

**Fig. 2.** MDCT angiography and BB MR analysis. The degree of luminal stenosis in the carotid arteries was evaluated from axial images and curved multiplanar reconstruction following NASCET criteria (**A**, **C**). After identifying the atherosclerotic lesions, serial cross-sectional images of the carotid arteries were obtained by altering the z-axis to allow analysis of the nearest distal (**B**) and proximal portions (**D**) without atherosclerotic plaque lesions. The outer vessel contour was manually traced to calculate the cross-sectional vessel area in each portion, and a mean reference CSA value was calculated. Plaque remodeling of carotid arteries was assessed using both RI and RR. On MRI, signal intensity of the plaque lesion of interest was calculated relative to the signal intensity to the sternocleidomastoid muscle on T1WI (**E**). At = Anterior; P = posterior; L = left; R = right.



lated as the ratio of CSA at the maximal vessel stenosis (measured from the luminal-intimal boundary to the outer vessel wall) to the mean reference CSA [17], and plaque RR, which was calculated as the ratio of CSA at the maximal vessel stenosis to the reference CSA in the distal portion [18].

RI = CSA at the point of maximum stenosis/mean of reference CSA

RR = CSA at the point of maximum stenosis/reference CSA at the distal portion

Positive remodeling or negative remodeling was defined on the basis of RI or RR: positive remodeling RI > 1.0; negative remodeling RI < 1.0; positive remodeling RR > 1.0, and negative remodeling RR < 1.0.

#### Magnetic Resonance Imaging

MRI was performed using a 1.5-tesla whole-body imager (Gyrosan Intra; Philips Medical Systems, Best, The Netherlands). Two types of MRI data were collected for each patient: (1) three-dimensional time of flight (3D-TOF) MR angiography (MRA), and (2) electrocardiogram (ECG)-gated BB images. 3D-TOF MRA was performed using 3D-T<sub>1</sub> fast-field echo sequence with an 8-channel SENSE neurovascular coil (5 cases) or Synergy Head/Neck coil

(8 cases). Scan parameters were as follows: repetition time (TR) 16–24 ms; echo time (TE) 3.7–6.9 ms; flip angle 18–22°; field of view (FOV) 170–1,200 mm; matrix 256–304 × 174–196, and slice thickness (Thk) 1.2–2.0 mm. BB T<sub>1</sub>-weighted imaging (T1WI) and T<sub>2</sub>-weighted imaging (T2WI) were performed using an ECG-gated double inversion recovery two-dimensional turbo spin-echo sequence with 8-channel SENSE neurovascular coil (4 cases) or small-diameter radiofrequency surface coil (2 cases). Parameters for BB T1WI were as follows: TR 750–1,200 ms; TE 14–17 ms; echo train length 7; FOV 160–200 mm; matrix 304 × 222–242, and Thk 3 mm. Parameters for BB T2WI were as follows: TR 1,500–2,400 ms; TE 70–80 ms; echo train length 17; FOV 160–200 mm; matrix 256–304 × 187–241, and Thk 3 mm. Chemical-selective fat saturation was applied to all BB sequences to reduce the signal from subcutaneous fat tissues. Zero-filled Fourier transformation was used to reduce pixel size, which ranged from 0.31 × 0.31 to 0.49 × 0.49 mm, depending on FOV, and to minimize partial-volume artifacts.

The most stenotic lesion was initially identified by 3D-TOF MRA. BB images were subsequently obtained in the transverse plane almost perpendicular to the long axis of the abnormal vessel. Slice levels were centered at the carotid bifurcation on the operative side in each patient. This protocol generated 3–9 image locations per patient examination.

#### Image Analysis

A manual operator-defined region of interest was drawn for each plaque to calculate the signal intensity relative to the ipsilateral sternocleidomastoid muscle on BB T1WI using the following formula (fig. 2E). Circular regions of interest between 5–10 mm<sup>2</sup> were placed on a workstation (Ziostation; by T.M.).

$$\text{Relative signal intensity (rSI)} = \frac{\text{signal intensity in plaque}}{\text{signal intensity in the sternocleidomastoid muscle}}$$

#### *Histological Grading of Carotid Artery Plaques Obtained by CEA*

Ten samples of lesions obtained by CEA were used to categorize and assess the histologic classification of atherosclerotic plaques. After surgery, the CEA specimens were fixed in 10% normal formaldehyde and cut into sequential 5-mm blocks, starting from the specimen base (the proximal or common carotid end) towards the bifurcation and beyond until the whole length of the specimen had been cut. Sections from each block were stained with hematoxylin and eosin. Complicated (type VI) plaques were graded using the following criteria: (1) free red blood cells within the intima or media not associated with the blood vessel lumen; (2) organized lamellar plaque or luminal adherent thrombosis (lines of Zahn, platelets, fibrin, red blood cells and white blood cells); (3) hemosiderin-containing macrophages, or (4) surface defects or rupture. On the basis of the above American Heart Association (AHA) criteria, 10 atherosclerotic plaques were classified into either stage VI or not by a single experienced neurosurgeon (H.K.) who was blinded to the clinical information.

#### *Biochemical Markers*

High-sensitivity C-reactive protein (hsCRP), hemoglobin A1C (HbA1C), total cholesterol, low-density lipoprotein cholesterol (LDL-C) and high-density lipoprotein cholesterol (HDL-C) levels were measured as follows: hsCRP by latex agglutination nephelometry; HbA1C by high-performance liquid chromatography; total cholesterol by enzyme reaction using N-ethyl-N-(2-hydroxy-3-sulfopropyl)-3,5-dimethoxyaniline sodium salt (DAOS method); HDL-C by direct measurement using cholesterol esterase, cholesterol oxidase and peroxidase, and LDL-C was indirectly calculated using the Friedewald formula. In the symptomatic group, data obtained within 7 days after the stroke event were selected.